INFRASTRUCTURE ROBOTICS: A TECHNOLOGY ENABLER FOR LUNAR IN-SITU RESOURCE UTILIZATION, HABITAT CONSTRUCTION AND MAINTENANCE

Nader Abu El Samid, Jekanthan Thangavelautham, Jim Richard, Dale Boucher and Gabriele M.T. D'Eleuterio

ABSTRACT

NASA's planned permanent return to the Moon by the year 2018 will demand advances in many technologies. Just as those pioneers who built a homestead in North America from abroad, it will be necessary to use the resources and materials available on the Moon, commonly referred to as in-situ resource utilization. This benefit would come in a number of ways. Required payloads would be smaller as supplies would be available at the mission site. This would allow for much less expensive missions as the launch fuel-to-payload weight ratio is greater than 9:1. In addition, this would free up valuable payload space for other instruments and tools, allowing more effective and higher-return missions to be undertaken.

Preparation would nonetheless be required well in advance of manned missions. In this concept study we put forward a role for robotic precursor missions that would prepare for the arrival of astronauts, serving to establish methods of collecting oxygen, water and various other critical resources. It will also be of principal importance to perform site preparation to set up a power generation center necessitating excavation of trenches, foundations, radiation shielding, landing and launch sites. We explore the potential role for autonomous, multirobot excavation solutions for these infrastructure development tasks. As part of this analysis, we compare various excavation platforms using an integrated real-time 3D dynamics simulator and autonomous control techniques for lunar surface interactions.

Traditional human-designed controllers lack the ability to adapt in-situ (without human intervention), particularly when faced with environmental uncertainties and changing mission priorities which were unaccounted for during design. By contrast, use of Artificial Neural Tissues (a machine learning approach) to produce autonomous controllers requires much less human supervision. These controllers only require a single global fitness function (akin to a system goal) and can perform autonomous task decomposition through a Darwinian selection process.

This novel quantitative approach combining real-time 3D simulation with machine learning provides an alternative to the often disputed and unreliable qualitative predictions of terrestrial excavation solutions applied to the lunar surface. Besides an autonomous infrastructure robotics concept, we also consider traditional approaches including teleoperated single and multirobotic systems. Some of the advantages of the autonomous multirobot approach to excavation over the traditional ones are analyzed in terms of launch mass, power, efficiency, reliability, verifiability and overall mission cost.

I. INTRODUCTION

NASA's planned permanent return to the Moon by the year 2018 will demand advances in many technologies. Just as those pioneers who built a homestead in North America from abroad, it will be necessary to use the resources and materials available on the Moon, commonly referred to as in-situ resource utilization. An important facet of lunar base construction will involve site preparation to set up a power generation center, habitat locations and other facilities requiring excavation of trenches, foundations, radiation shielding, landing and launch sites.

One option to accomplish the necessary site excavation tasks is to use a teleoperated or locally controlled construction vehicle driven by a single astronaut. The extensive use of astronauts for excavation and site preparation tasks poses human safety concerns. Furthermore, additional habitat infrastructure needs to be in place before base construction to support an astronaut construction crew. Other proposed approaches such as teleoperation of multiple vehicles using a single operator requires a scheduling system and communication infrastructure. However saturation limits the number of tasks that can be handled by a human operator [1] making it less efficient than a fully autonomous solution that operates continuously. Building upon traditional human operated digging equipment like bulldozers, use of autonomous robotics solutions to perform infrastructure development tasks are the logical next step, and could yield significant benefits in terms of system performance measures such as cost, launch mass, overall system complexity, length of mission, safety and other relevant mission objectives.

In this paper, lunar base construction will be analyzed from a system wide stance and will include applying sets of excavation and construction equipment representative of options described in literature. Consensus among mission planners has yet to be achieved regarding the major objectives in

This work was funded in part by the National Science and Engineering Research Council. Nader Abu El Samid (n.abuelsamid@utoronto.ca), Jekanthan Thangavelautham and Gabriele D'Eleuterio are with the department of Aerospace Engineering, University of Toronto Institute for Aerospace Studies, Toronto, Canada. Jim Richard is with Electric Vehicle Controllers Ltd., Sudbury, Ontario, Canada and Dale Boucher is with the Northern Center for Advanced Technology Inc, Sudbury, Ontario, Canada.

a lunar base construction mission, with many competing proposals put forward over the years. The mission selected in Boles *et al.* [2], and the analysis technique used to evaluate lunar base construction methods are chosen as a basis for this paper.

One of the major hurdles with lunar base construction is that lunar surface condition (apart from the previous Apollo and Luna mission landing sites) are not well understood and are subject to a high degree of uncertainty. In the study performed by Boles *et al.* [2], excavation related construction tasks were identified as one of the key areas where improved ground site information and improvements in control strategies are predicted to yield significant reductions in total earth-launch mass (the most important factor affecting overall mission cost). However one limitation with the Boles *et al.* study is that a panel of experts was used to determine construction efficiency rates (referred to nominal rates of production). The use of experts, rather than actual simulations or hardware testing, to derive efficiency rates is subjective and amplifies the already high uncertainty associated with lunar construction. In addition, the work focused exclusively on astronaut-operated control approaches (as opposed to autonomous robotic systems) for excavation tasks. An objective of this paper is to obtain actual productivity data estimates using high fidelity dynamics simulations combined with an autonomous control strategy for excavation (generated using adaptive machine learning techniques). The goal of this paper is to determine whether autonomous, multirobot infrastructure robotics solutions have advantages over teleoperated or manual approaches. Any advantages shown over the techniques proposed by Boles *et al.* would satisfy this objective.

For the autonomous strategies considered in this paper, a machine learning approach called the Artificial Neural Tissue (ANT) framework [3], [4], [5] is used to perform excavation tasks. This machine learning method is used to 'breed' for robotic controllers in an artificial Darwinian manner. For the excavation and site preparation tasks (a key components of any infrastructure development activity), ANT can produce controllers that interpret and follow excavation blueprints, can successfully avoid obstacles, perform layered digging, avoid burying or trapping other robots, perform coordinated group actions and clear/maintain excavation routes, all with minimal task-specific assumptions and supervision. Furthermore, since little preprogrammed knowledge is given, ANT may discover novel solutions that otherwise maybe overlooked by a human designer. Performance comparison of these autonomous multirobot excavation strategies relative to manual approaches is performed in simulation, using Digital Spaces, a real-time 3D dynamics simulator [6], [7].

In this paper, a cyclic decision theory approach is first described that highlights areas where further research can reduce the cost of lunar base construction. This is followed by explanation of the simulation experiments, used to find nominal rates of production with details on the ANT controller used for autonomous multirobot excavation. In addition, a brief overview of the newly implemented deformable terrain model used within the Digital Spaces 3D realtime dynamic simulator for the ANT excavation experiments is presented. A discussion section follows, outlining mission level comparisons between complete teleoperated solutions from literature and the proposed autonomous multirobot excavation solutions. The paper ends with a summary outlining mission-level benefits of using autonomous multirobot excavation solutions over traditional approaches and future work.

II. Background

Much of the literature discussing lunar base construction focuses on the tasks and equipment required, with a tendency to rely on 'nominal data' estimates under terrestrial conditions. A paper by Shimizu Corp. looks at excavation tasks from an energy standpoint, but uses terrestrial numbers to determine total requirements [8]. Depending on equipment, productivity rates can differ substantially between the earth and the moon and that would play an important role in calculating total energy. Also, the study does not account for differing net production rates during the various phases of lunar base construction. Specialized vehicles such as bulldozers used for clearing type tasks maybe used extensively during the early phases of the mission. However the production rates of these vehicles are expected to differ from other vehicles used predominantly in later phases such as a front loader (used for short range hauling).

Other studies focus on detailed equipment design [9], and relative comparison of concepts based on trade studies. Some put emphasis on the prime movers and lifting equipment, without analyzing excavation tasks in lunar terrain [10]. A recent trade study by NASA compares excavation equipment based on the expected ability for them to handle the different types of digging tasks faced on the moon [11]. This includes qualitative assessment of criteria such as mining and construction productivity, digging capability, reliability, and maintainability. Although productivity details are highly uncertain, this analysis is useful in that it narrows down the options in a logical manner, paving the way for testing a smaller list of concepts under expected lunar conditions. Design configurations used in this paper are based on the candidate solutions proposed in these trade studies.

Traditional excavation technologies tend to have similar kinematic configurations to industrial robots, and excavation activities tends to consist of repetitive tasks making them potential candidates for automation. Motion control of a scoop through soil has been demonstrated along a desired trajectory using position accommodation and compliance control [12]. Utilization of robotics technology and automation in excavation applications would not only provide opportunities to maximize machine utilization and throughput, it would reduce the need for skilled operators and reduce the workload on remaining operators to ensure quality excavation results.

Elaborating on the potential use of robotic technologies, introducing a robot collective to accomplish the required task may be beneficial. In nature, ants digging tunnels to form a nest [13], has inspired researchers [14] to conduct

experiments using collective intelligence as a means of resolving the excavation problem. Rather than commanding one large and complex robot to perform the excavation, a team of smaller robots performing the task may help lower complexity and overall system cost. The ANT framework is a practical multirobot implementation of this concept, and applied in this paper to test the candidate equipment.

Since cost of prototyping and performing physical tests on actual excavators is very high, approaches that make use of simulation in an environment that accurately represents the moon would be practical. Digital Space Corporation's realtime 3D dynamic simulator, complete with deformable terrain modeling to simulate tool-regolith interactions and wheel/track-regolith modeling for tractive forces developed in the Space Robotics laboratory at the University of Toronto Institute for Aerospace Studies, represents a leap in simulation capability that makes such lunar tests possible.

The paper by Boles *et al.*, although subjective in some respects because of a reliance on experts rather than simulation or hardware testing to identify production rates for all aspects of the lunar construction project, can be extended because it specifically outlines a quantitative, robust model upon which to judge lunar base construction, complete with results for detailed teleoperated system options. The paper also states that digging tasks and equipment have the highest impact on total cost of a lunar base construction mission, suggesting that improvements in this area could be very beneficial for 'big picture' planning. Applying simulation results for alternative solutions to the problem into the model, and determining the impacts on mission design could lead to significant enhancements to any proposed mission.

In the following section, we start by considering a detailed mission manifest proposed in a case study by NASA [15]. An approach to assess lunar base construction is next described that 1) Identifies general tasks, and quantities of work for lunar base construction 2) Defines the resources required 3) Determines productivity 3) Uses deterministic and probabilistic sensitivity analysis on-key variables that affect mission cost and 4) Finds competitive alternatives.

III. Analysis

A research approach that uses decision tools to test competitiveness of alternative construction methods and equipment is described. The analysis technique uses decision theory that highlights areas where lowering uncertainty has benefits in terms of lunar base mission cost. The process begins by identifying some measure by which to assess sets of alternatives for equipment and methods required to build a lunar base. Next, data requirements for the decision approach are divided into 1) work to be completed; 2) resources available to do work, and 3) productivity and support needs for those resources.

The process, as described by Boles *et al.*, then follows cyclical steps, with three main phases: 1) deterministic: 2) probabilistic and 3) informational. Only the first two phases are used to assess competitiveness of alternatives, and are presented in this paper. The informational phase helps determine whether further reduction in uncertainty of key variables would be worthwhile. At the present time, additional reduction of uncertainty would require precursor exploratory missions to the moon to obtain detailed lunar site data. Thus, the informational phase is not pursued here. In Boles' *et al.* study however, digging tasks were identified in the informational phase as a potential area where accurate information would benefit lunar mission cost analysis. In this paper, the introduction of simulations to test automated solutions allows for a second iteration of the decision cycle to proceed, allowing for more accurate data extraction of excavation productivity rates. For the next iteration, fundamental improvements in reliability of basic data like regolith properties would be needed. A diagrammatic representation of the decision cycle is shown:

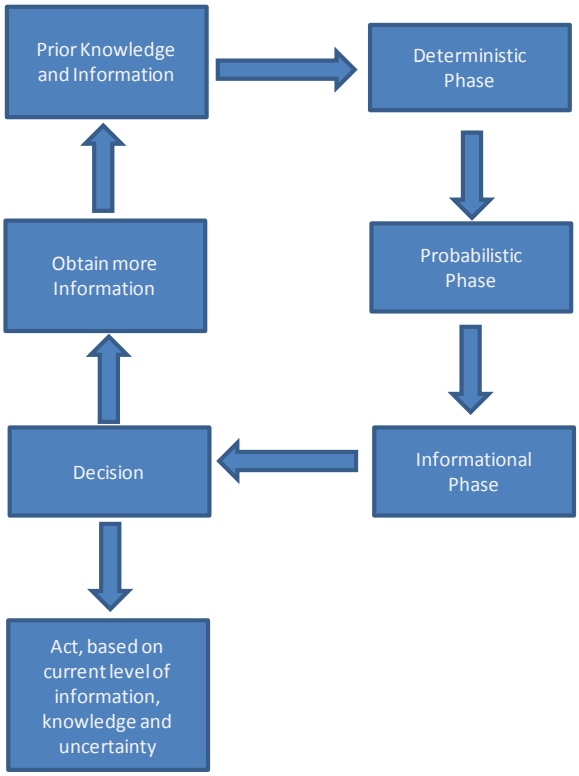

Fig. 1. Decision Analysis Cycle

A. Alternative Selection

This section explains various mission options considered in this paper. Based on a NASA case study[15] investigating a lunar base construction mission, generic sets of tasks and quantities of work are defined. In addition, alternatives representing lunar construction equipment cited in literature are produced. Design requirements taken into consideration include: 1) Ability to excavate the type of lunar regolith expected at the mission site; 2) Critical systems operating long term and reliably 3) Noesis to survive and operate in dusty environments; 4) Efficient power transmission and

utilization; 5) Maneuverability in majority of lunar terrain; 6) Packageability and landability of the rover system.

The mission design process outlined by Boles *et al.* also takes into account cost and maintenance factors pertaining to the excavation equipment. However, these factors were obtained through qualitative expert opinions. In this paper we develop simulations experiments for the various robotic excavation robots and come up with more accurate quantitative data used to arrive at key cost variables such as total earth-launch mass. Parameters used to define each piece of equipment are shown in Table I. Hardware reliability is incorporated into Maintenance Intra-Vehicular Activity (IVA), Maintenance Extra-Vehicular Activity (EVA), Rebuild IVA, Rebuild EVA, and maintenance resupply mass.

TABLE I
EQUIPMENT VARIABLES

Variable	Units
Power	Kilowatts
Mass	Metric Tons
Life	Hours of Operation
Maintenance Resupply	Metric Tons Over Life
Maintenance IVA	Crew Hours
Maintenance EVA	Crew Hours
Salvage Mass	Metric Tons
Rebuild IVA	Percent of Maintenance IVA
Rebuild EVA	Percent of Maintenance EVA

A total of 12 general cases have been assembled and analyzed, all with basic lifting, digging and hauling capabilities. Alternatives 1 to 9 are described in detail in [14] and shown in Figure 2-4. Options 1 to 5 represent manually operated, terrestrial-based construction systems, and are extended to incorporate multirobot, autonomous excavation capability (Figure 2). The Legged platforms and super crane concepts are manually operated and are considered for options 6 to 9 (Figure 3). Furthermore, these options are extended to include autonomous, multirobot approaches (alternative 1 is used as a template) with excavation equipment substituted as shown in Figure 4. System variations are shown in Figure 5, with the legend provided in Figure 6. An autonomous version of the single 8 ton excavator in alternative 1 was also tested in Digital Spaces, and comparisons made against the multirobot bulldozer, front loader and bucket wheel options.

Images of the simulated tracked front loader and 6 wheel bulldozer configurations are shown in Figures 7 and 8. The track vehicle platform design is based on pre-phase A design work for NASA's proposed Robotic Lunar Exploration Program surface mission [16]. The 6 wheel vehicle dozer is based on a vehicle designed and constructed by the Northern Centre for Advanced Technology Inc. (NORCAT), Electric Vehicle Controllers Ltd. (EVC), and the space robotics group at the University of Toronto.

These alternatives are tested in simulation using an Artificial Neural Tissue control architecture, which is discussed in Section IV.

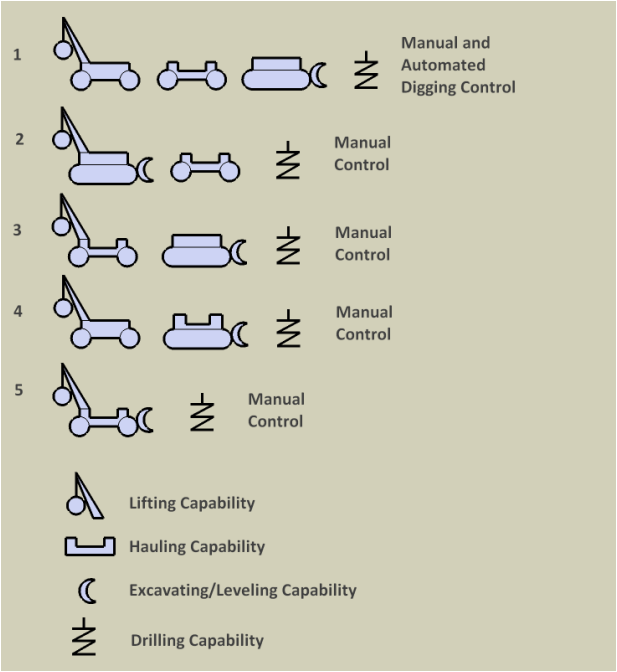

Fig. 2. Alternatives 1-5

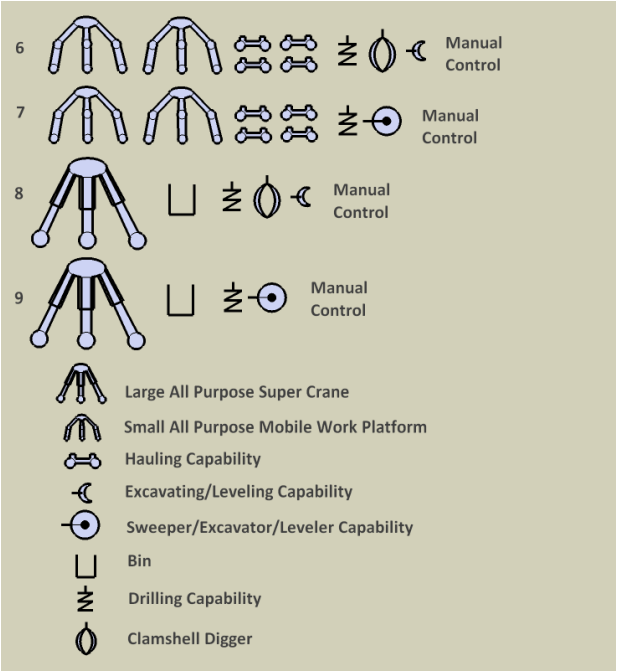

Fig. 3. Alternatives 6-9

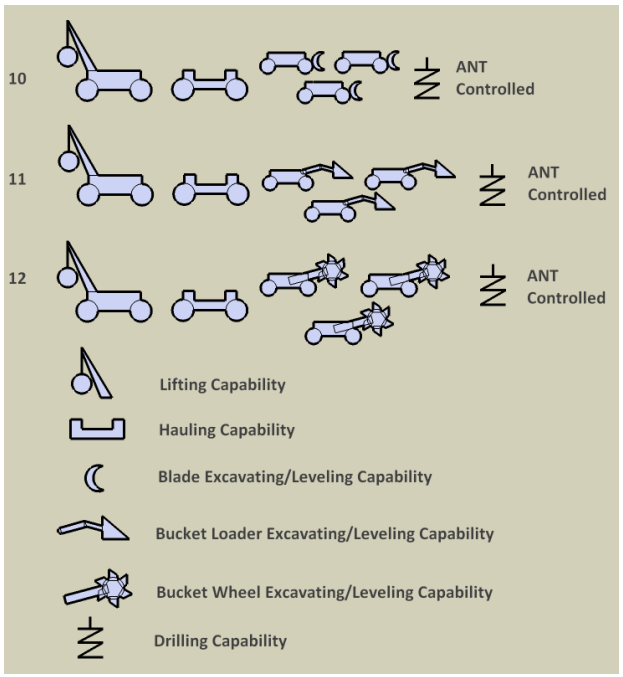

Fig. 4. Alternatives 10-12

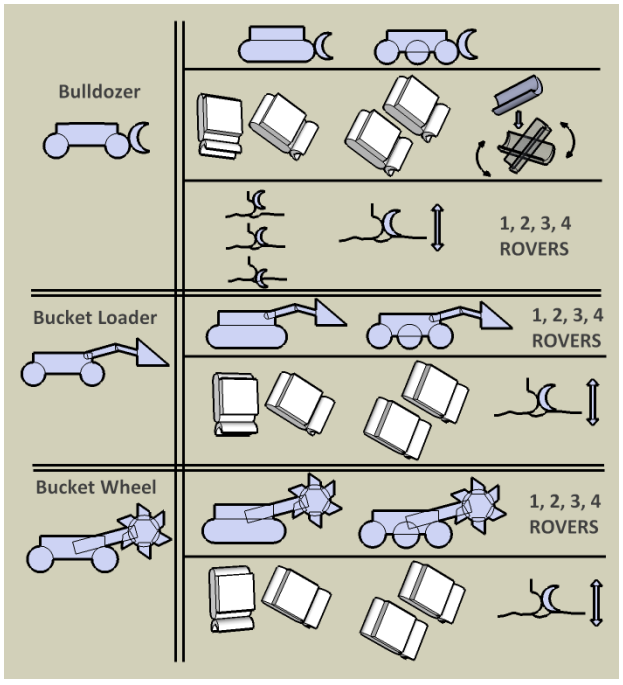

Fig. 5. Variations Applied to Alternatives 10-12

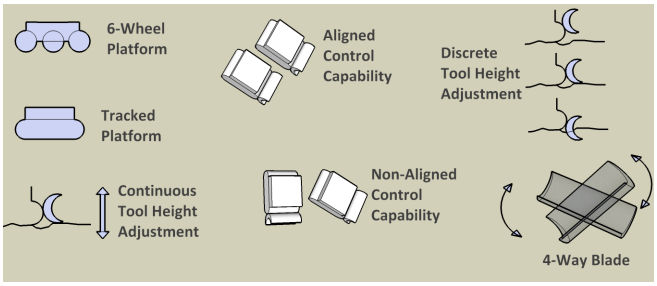

Fig. 6. Legend of Variations

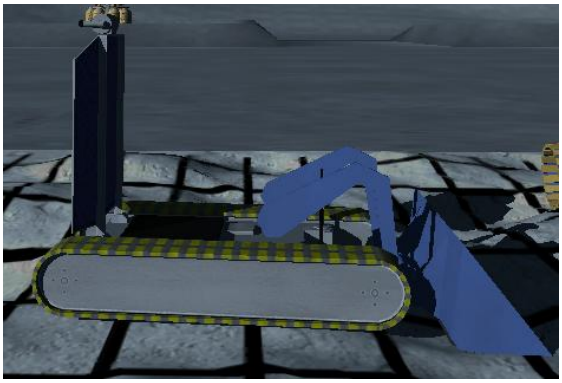

Fig. 7. Tracked Bucket Loader

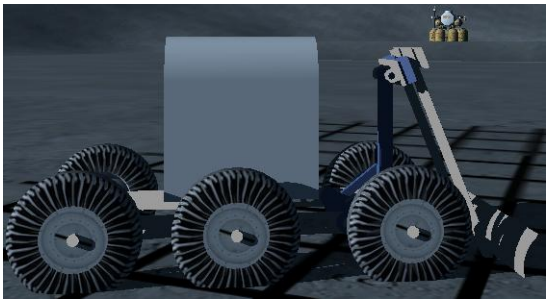

Fig. 8. 6-wheel Bulldozer

B. Total Earth-Launch Mass and Key Resource Variables

Total earth-launch mass, the most logical performance variable to assess competitiveness of lunar base construction methods, is used as the figure of merit in this paper. It should also be noted that the total earth-launch mass is found to be the most biggest cost component in the process of lunar base construction [2]. The calculation consists of crew and equipment allocations, and is the most effective way of determining transportation costs, and in turn the total cost of constructing a lunar base.

A mathematical model for total earth-launch mass, the performance measure used to compare alternatives, is developed with the aid of an influence diagram [14]. The initial launch mass of basic equipment, maintenance resupply launch mass, and replacement launch mass make up total equipment launch mass. Life sustenance needs such as water, food, clothing etc. make up crew-consumables

launch mass. The construction-related earth-launch mass, from [14] is as follows:

$$\sum_{\text{(all machines)}} M_i \cdot \#_i + C_i \cdot R_i + INT(C_i - \#_i)(M_i - S_i) + \left\{ \frac{7M_D \left[EVA + \sum_{\text{(all machines)}} C_i \cdot MEVA_i + INT(C_i - \#_i)(REVA_i) \right]}{H_{EVA} \cdot D} \right\} + \left\{ \frac{7M_D \left[IVA + \sum_{\text{(all machines)}} C_i \cdot MIVA_i + INT(C_i - \#_i)(RIVA_i) \right]}{H_{IVA} \cdot D} \right\} \quad (1)$$

Where

$$C_i = \sum_{\text{(all tasks)}} \frac{Q_j}{P_j}(N_{ij})(A\%_{ij})/Life_i \quad (2)$$

$$EVA = \sum_{\text{(all tasks)}} \frac{Q_j}{P_j}(NEVA_j)(A\%EVA_j) \quad (3)$$

$$IVA = \sum_{\text{(all tasks)}} \frac{Q_j}{P_j}(NIVA_j)(A\%IVA_j) \quad (4)$$

The first summation represents hardware launch mass, and the final two summations are the crew consumables. Variable definitions for the launch mass formula are provided in the appendix.

C. Deterministic Model Phase

The deterministic model phase involves performing sensitivity analysis to highlight the most influential variables impacting the mission. Using productivity rates established from simulation results for each design scenario, a summation over all tasks of the estimated quantities of work divided by production rates of the necessary resource produces the total number of hours required for each generic task. Minimum and maximum values for each rate are used to determine model sensitivity. The five most influential variables impacting mission costs for all possible system alternatives are shown in Table II. Leveling tasks, such as road clearing and creating landing/launch pads, involve flattening out uneven terrain. Excavating tasks on the other hand involve digging out deep holes used for habitat foundations or burying nuclear reactors. For crew-only construction tasks which cannot be simulated, estimates on the productivity data are obtained from literature. After adjusting the variables using deterministic maximums and minimums, no particular alternative was observed to be entirely dominant. Use of additional probabilistic analysis on these sensitive variables, through the mathematical encoding of risk and uncertainty, can identify these alternatives with the available information.

TABLE II
SENSITIVE VARIABLES

Alternatives 1-5, 10-12	Alternative 6	Alternative 7	Alternative 8	Alternative 9
Level	Level	Level	Level	Level
Excavator Life	Excavate	Excavate	Excavate	Excavate
Excavate	Mobile Work Platform Life	Elevate Regolith	Elevate Regolith	Elevate Regolith
Elevate Regolith	Elevate Regolith	Mobile Work Platform Life	Back-fill	Back-fill
Excavator Resupply	Blade Life	Boles Lunar Excavator Life	Super Crane Mass	Super Crane Mass

D. Probabilistic Sensitivity Analysis Phase

Probabilistic sensitivity analysis is a good tool to test competitiveness of alternatives. This process first involves encoding the probability distributions for the key variables highlighted in the deterministic analysis. True shapes of the probability distributions for the uncertain variables cannot be known with limited understanding of lunar site conditions. However, in many cases, a beta distribution is assumed [17]:

$$K(x-a)^{\alpha}(b-x)^{\beta}, a \leq x \geq b; a, b \geq -1 \quad (5)$$

Boles *et al.* relies on a minimum three data points required for PERT (Program Review and Evaluation Technique) analysis where durations of tasks are estimated as minimum, most likely, and maximum. Additional details on how dispersion of the distribution is obtained can be found in [18]. A cumulative probability curve is produced for each distribution, and discretized at 25%, 50%, and 25% intervals. The expected values from these ranges are fed into a decision tree, with five levels of the tree corresponding to the five sensitive variables for each alternative. An abbreviated tree is shown in Figure 9. The leveling time sensitive variable is shown as an example showing typical values and probabilities used in generating the decision tree.

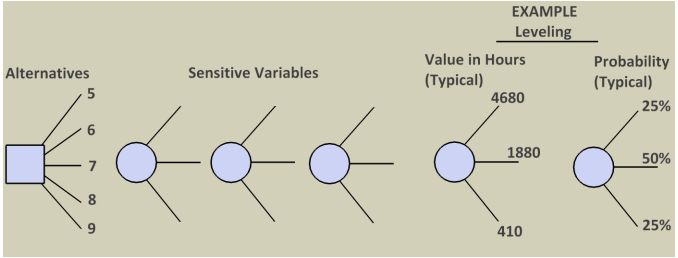

Fig. 9. Abbreviated Decision Tree

Next, the analysis involves adjusting the probabilities of each key variable (between 0% to 100% of the upper discretized expected value) in the decision tree. Consider the behaviour of alternative 5 as an example (over most of its range of possible values), where the total earth-launch mass is higher than all other cases. So based on leveling task

productivity, one can conclude that alternative 5 is uncompetitive, because of the high mission cost (see Figure 10). Furthermore, the best lunar base construction solution is identified by systematic analysis of all the sensitive variables using this procedure.

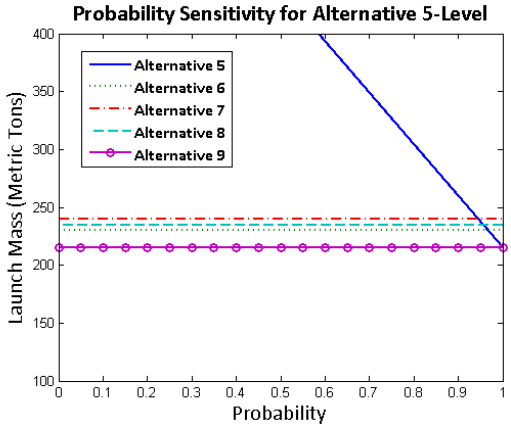

Fig. 10. Probabilistic Sensitivity of Alternative 5, Leveling Productivity

E. Digital Spaces Simulation Environment

The Digital Spaces simulation is divided into three major parts: 1) the Agent and Poser File; and 2) the deformable terrain model, which are all explained in the following subsections.

1) The Agent and Poser File: Each vehicle within the ANT simulation in Digital Spaces is defined as an agent. The agent is composed of all of the pieces that make up the rover, and the agent file contains configuration information of for all of the pieces. A poser script file is necessary to control each vehicle agent in the space. The defined behaviour functions can either manipulate the entire agent or individual joints

2) Deformable Terrain Model: The simulated lunar terrain is divided up into rectangular boxes, representing regolith containers, which rise and fall to reflect appropriate interaction with the excavation tool. When the bucket shape in the simulator comes into contact with one of these boxes, a volumetric friction file that computes the Balovnev forces acting on the blade is executed. The variables that change dynamically during excavation, affecting the force on the blade, are tool depth, d and blade rake angle, β (see Figure 24).

The horizontal, vertical and total forces acting on the bucket are provided in the Appendix. Figure 12 shows Balovnev draw bar force variation with tool depth.

Volume conservation is also applied on the terrain to produce realistic deformation. When the blade passes through a terrain box, that box gets lowered to reflect the blade's average depth. The total volume removed is correspondingly added to the terrain boxes directly ahead, representing proper accumulation of regolith in front of the blade.

Wheel/Track interaction with the terrain is also modeled, with analytical calculations performed to established all appropriate components of traction. The calculated traction

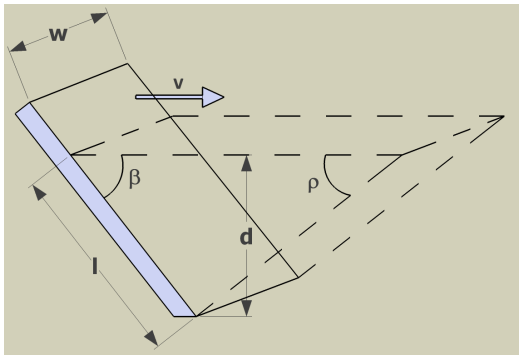

Fig. 11. Cutting Operation Variables

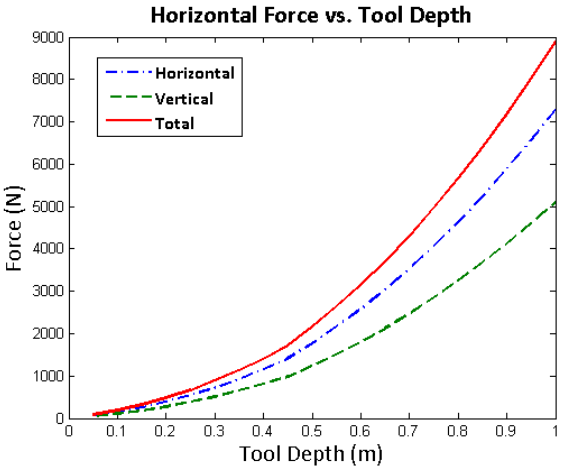

Fig. 12. Balovnev Drawbar Force Variation with Tool Depth

forces are converted into force vectors in the simulator, and are applied to the wheels to achieve correct vehicle response. The effects of slippage, sinkage, bulldozing resistance, resistances to obstacles, and lunar gravity effects are all determined and matched to results from Figure 13.

IV. Simulation Experiments

Two types of experimental simulation are used in this study. The first simulator is modeled as a low-fidelity grid world environment in two-dimensions, and is used to evolve (train) the controller for the digging task. Training is accomplished by a providing an objective (fitness) function used for selection of candidates solution in a Darwinian manner. The intention is for the training algorithm to finding candidate solutions that maximize this objective function under different scenarios. The objective (fitness) function f for the excavation task is:

$$f = \frac{\sum_{j=1}^{J}\sum_{i=1}^{I}\left(p_{i,j}\cdot e^{-2|g_{i,j}-h_{i,j}|}\right)}{\sum_{j=1}^{J}\sum_{i=1}^{I}p_{i,j}} \tag{6}$$

Workspace dimensions are I and J, with $\sum_{j=1}^{J}\sum_{i=1}^{I}p_{i,j} > 0$ and $p_{i,j} = 1$ if the terrain box i,j requires excavation, and 0 otherwise; target depth is $g_{i,j}$ and current regolith depth is $h_{i,j}$. A description of each

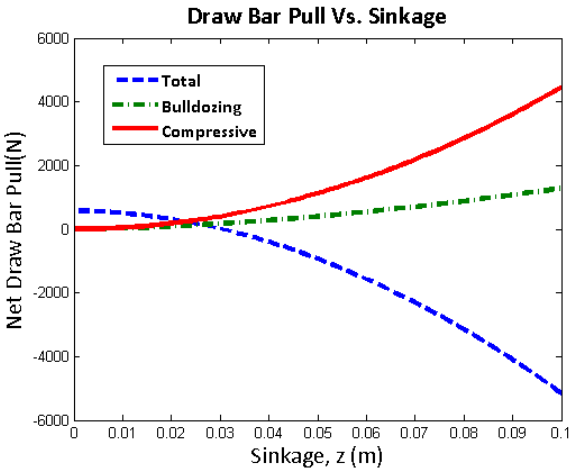

Fig. 13. Drawbar Pull as a Function of Sinkage

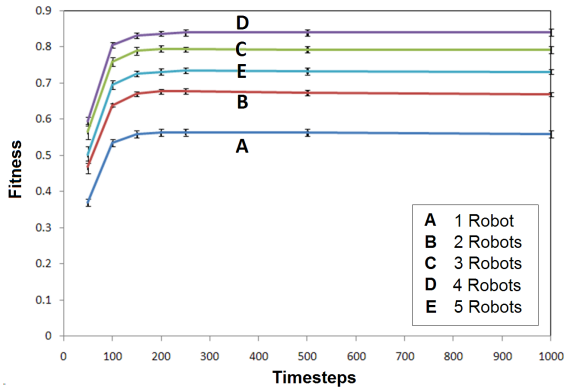

Fig. 14. Fitness vs. Time: Training Simulator

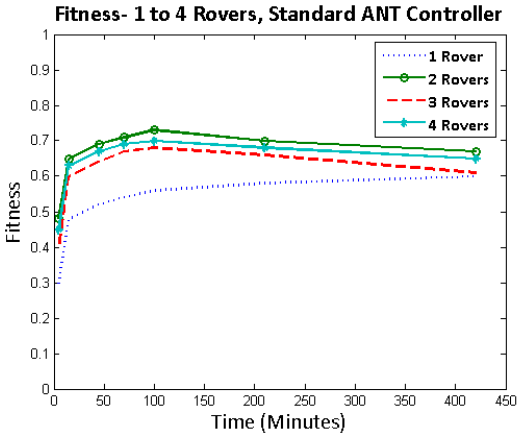

Fig. 15. Fitness vs. Time: Digital Spaces Simulation

simulated robot in the grid world environment is shown in Appendix. Each robot is given access to set of sensory inputs (Table VII, Figure 21) and trigger a set of basis behaviours (Table VIII). The ANT controllers are expected to interpret excavation blueprints and accomplish subtasks including performing layered digging and leveling excavation routes. The excavation blueprints are provided in the form of a goal map to each robot controller and it specifies the target depth of the excavation area and identifies dumping areas [5]. In addition to previously published excavation capabilities, the ANT controllers considered for this study can also perform group actions while in alignment, such as excavation of an area in a line configuration (Figure 16- 19).

Once the controllers have acquired the necessary traits for accomplishing the excavation tasks from the evolutionary training procedure, they are ported into the higher-fidelity Digital Spaces simulation environment for further validation. Robotic hardware can be represented with increased fidelity, complete with sensor interfacing, and with integrated deformable terrain modeling. Deformable terrain modeling allows for realistic regolith-tool and wheel/track-terrain interactions. Steps in this virtual approach facilitate prototyping and testing of alternative digging concepts and can potentially reduce hardware experiment costs. With the iterative approach described in this paper, a single best approach developed in simulation can then be constructed in hardware for further validation.

To ensure consistency between the training simulation and the Digital Spaces virtual world, fitness is monitored for 1, 2, 3, and 4 bulldozer simulations with the alignment capable ANT controller. The results are shown in Figures 14 and 15. The main work area goal map dimensions used for all simulation experiments in this study is $8 \times 8 \times 1.5$ m deep.

Evaluation of ANT controller fitness shows that both simulators correlate very well to one another over the time it takes to complete a task. After reaching peak fitness at about 100 minutes for all except the single rover solution, the fitness drops gradually in the Digital Spaces results. The training simulator results level off after about 200 timesteps. The reason for the drop is that after the final goal depth is achieved, the vehicles continue to move around the work area with blade height set to level. Theoretically, this means the rovers do not dig any regolith, but in reality, they skim small amounts of material off, going slightly below the goal depth over time.

V. Results and Discussion

TABLE IV
Deterministic and Probabilistic Launch Mass for Earthmoving Specific Tasks (Metric Tons)

Alternative	Deterministic	Probabilistic
1 (ANT Controlled)	16.46	28.66
10 (1 rover)	6.52	11.08
10 (2 rovers)	5.26	7.39
10 (3 rovers)	3.56	5.91
10 (4 rovers)	4.12	6.88
11 (3 rovers)	3.66	5.99
12 (3 rovers)	3.63	5.94

Deterministic launch mass for the alternatives is presented in Table III. Alternatives 1 to 9, are listed along with the three-rover ANT controlled variations of the bulldozer, bucket loader and bucket wheel configurations. The three

TABLE III
EARTH-LAUNCH MASS BREAKDOWN DETERMINISTIC RESULTS (METRIC TONS)

Alternative	Description	Crew Consumables	Equipment	Total
1a	Manually Operated 8 Ton Bulldozer	103.69	154.91	258.60
1b	ANT Controlled 8 Ton Bulldozer	43.95	53.32	97.27
2	Manually Operated Crane-Bulldozer	114.50	154.39	268.89
3	Manually Operated Truck-Bulldozer	112.37	167.21	279.58
4	Manually Operated Crane-Truck	99.63	154.44	254.07
5	Manually Operated Crane-Dozer-Truck	110.04	118.51	228.55
6	Manually Operated Mobile Digger	125.61	39.86	165.47
7	Manually Operated Mobile + Boles Excavator	100.88	48.65	149.53
8	Manually Operated Super Crane Digger	96.32	46.78	143.10
9	Manually Operated Super Crane + Boles Excavator	85.16	37.82	122.98
10	ANT Controlled Bulldozer	30.93	53.45	84.38
11	ANT Controlled Front Loader	30.99	53.49	84.48
12	ANT Controlled Bucketwheel	30.97	53.47	84.44

rover cases have the lowest total earth-launch masses out of all other multirobot scenarios, and are listed in Table III. The bulldozer option 10, relative to all other cases, has the lowest launch mass. This alternative utilizes: 1) continuous blade adjustment for constant level digging; 2) 4 way blade control; 3) 4 wheel configuration; and 4) boom and bucket similar to the front loader configuration to perform bulldozing. Four way blade control, combined with continuous blade adjustment, gives this dozer configuration the ability to sculpt the work area to any arbitrary goal map, and adjust angle quickly, resulting in negligible drop in digging productivity. A human operator on the other hand, as discussed in Boles *et al.* [2], takes time to angle the tool correctly, and slows the process. In addition the four-wheel configuration is also found the lightest of all options.

The front loader and bucket wheel using autonomous ANT controller have slightly lower total earth-launch mass in comparison to the bulldozer because of slightly lower digging productivity. The bucket loader configuration spends non-productive time moving to and from dump sites with it's full bucket elevated, and does not dig during these times, and so has overall lower digging productivity than the bulldozing and bucket wheel approaches. The bucket wheel has constraints on bucket size due to high excavation forces that can form on the tool blades, and corresponding limits on motor power available to turn the bucket wheel itself. The limits on bucket size, lower nominal digging rates, and hence overall launch mass is higher than bulldozing, but not lower than the front loader option.

It should also be noted that the autonomous ANT controller configurations are only used for mobile excavation activity while lifting, drilling, and transportation capability is assumed to be teleoperated (similar to alternatives 1 to 9). Because the vehicle sizes used for bulldozer, front loader and bucket wheel are generally similar, and all have high nominal digging productivities (above 25 m^3/hour- see Table V), the end observed effect is that there is no substantial difference in total earth-launch mass between the alternatives that use the autonomous controllers. However, significant improvement is observed for the autonomous solutions over the teleoperated approaches. By looking at earth-launch mass of the excavation resources alone, the differences between autonomous solutions become more apparent. Table IV shows deterministic and probabilistic launch mass of the digging resources alone for the autonomous alternatives.

TABLE V
DETERMINISTIC SIMULATED EXCAVATION AND LEVELING TASK PRODUCTIVITY DATA (M^3/HOUR)

Task	Maximum	Expected	Minimum
ANT Controlled Bulldozer (3 rover solution)			
Excavate	78.3	47.49	1.67
Level	78.3	63.32	1.67
ANT Controlled Bucket Loader (3 rover solution)			
Excavate	42.28	26.62	1.67
Level	42.28	35.50	1.67
ANT Controlled Bucketwheel (3 rover solution)			
Excavate	49.91	31.43	1.67
Level	49.92	41.91	1.67

A significant reduction in mass occurs when the number of robots is increased from one to three, but then the mass rises with further increase in the number of robots. With too many robots in a limited area, digging productivity drops due to factors such as *antagonism*, where one robot undoes the actions of another. The end effect is reduced productivity and thus high launch mass because of higher maintenance and rebuilding costs. The best solution for the bucket loader and bucketwheel configurations is to use three robots for a 8×8 meter excavation site. Figure 16 to 19 shows snapshots of three front loaders performing autonomous excavation using the ANT controller. The vehicles learn to arrange themselves (and move) in a line as shown to increase

excavation efficiency.

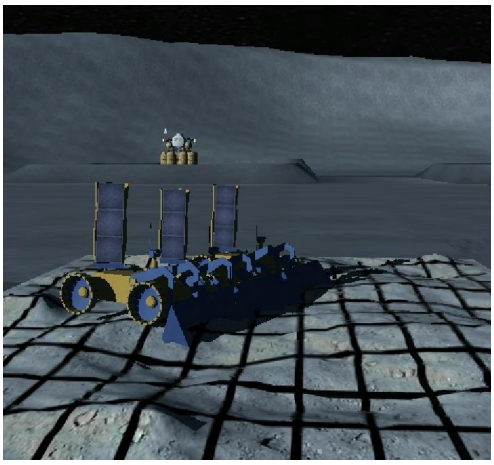

Fig. 16. Three rover aligned bulldozing simulation: after 5 minutes

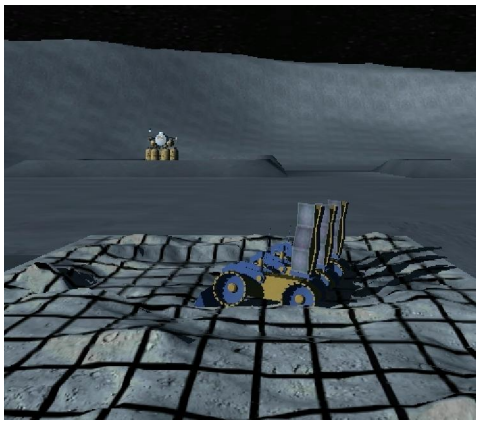

Fig. 17. Three rover aligned bulldozing simulation: After 45 minutes

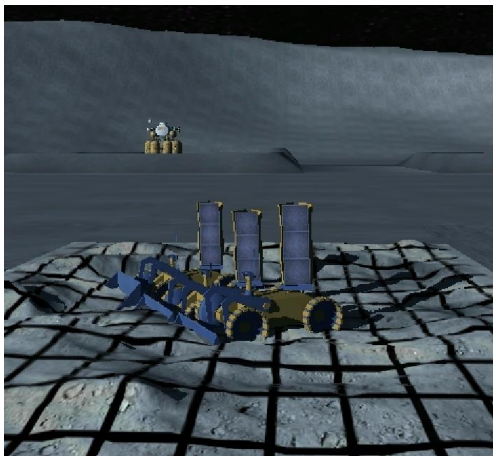

Fig. 18. Three rover aligned bulldozing simulation: After 130 minutes

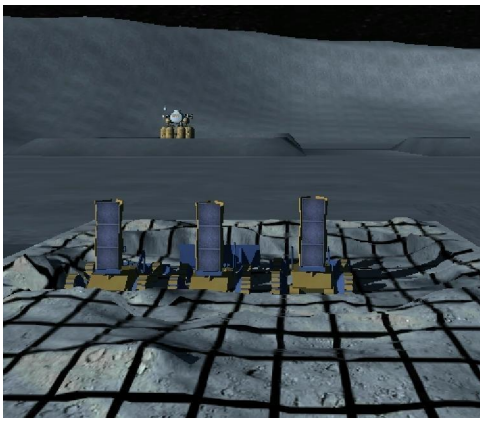

Fig. 19. Three rover aligned bulldozing simulation: After 300 minutes

In general, equipment costs for automated solutions are lower compared with the manual approaches suggested in [14], contributing to the launch mass reduction. In addition, many factors contributing to productivity reduction of manually operated approaches on the moon are not factors for ANT controlled systems. The obvious one would be that a driver is not needed for the autonomous vehicle, so constraints put on productivity due to work day duration and crew productivity limits do not play a role here. Additional time spent by human operators to readjust blade or bucket height in order to contour the terrain to the desired shape is not needed, because the blade or bucket is continuously adjusted by the autonomous controllers. The elimination of these factors for the autonomous solution results in increased productivity.

The Boles *et al.* model also contains a quantitative deterministic approach for measuring model robustness. This involves varying some basic parameters in the model and determining whether the rankings of the alternatives remain consistent [14]. Extensive analysis was conducted by adjusting quantities of work, EVA and IVA hours per day and crew consumption rates and results is shown in Figure 20. Performing this sensitivity analysis (from 0% to 100% chance of experiencing its uppermost expected value, for each of the key variables affecting total earth-launch mass) on all alternatives further confirms that the bulldozing alternative is the most competitive of all.

The cost of delivering resources to the moon is substantial, and a significant reduction in launch mass as shown for the autonomous solutions will lead to sizable cost savings. We also compare the alternatives presented in this paper in terms of number of rocket launches (assuming an Ares V launch vehicle) in Table VI. The Ares V launch vehicle has a payload capacity of 71 metric tons to the moon [19] and furthermore we budget a 20% mass margin to the deterministic launch masses presented earlier. For the autonomous solutions (alternatives 10 to 12), the number of rocket launches stands at 2, that is 2 lower than the manually controlled alternatives 1 to 5, and 1 fewer than options 6 to 9.

VI. CONCLUSIONS

Higher fidelity simulation experiments of lunar excavation tasks using autonomous controllers show much higher pro-

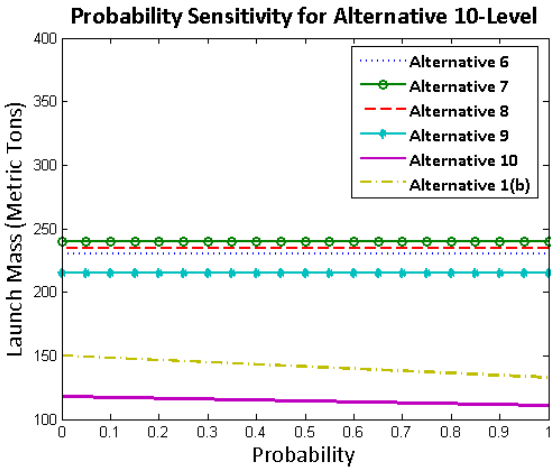

Fig. 20. Probabilistic Sensitivity Graph- Alternative 10 Launch Mass Competitiveness is shown with Respect to Leveling Productivity

TABLE VI

NUMBER OF ROCKET LAUNCHES REQUIRED FOR ALTERNATIVES

Alternative	Description	Launches
1a	Manually Operated 8 Ton Bulldozer	4
1b	ANT Controlled 8 Ton Bulldozer	2
2	Manually Operated Crane-Bulldozer	4
3	Manually Operated Truck-Bulldozer	4
4	Manually Operated Crane-Truck	4
5	Manually Operated Crane-Dozer-Truck	4
6	Manually Operated Mobile Digger	3
7	Manually Operated Mobile + Boles Excavator	3
8	Manually Operated Super Crane Digger	3
9	Manually Operated Super Crane + Boles Excavator	3
10	ANT Controlled Bulldozer	2
11	ANT Controlled Bucket Loader	2
12	ANT Controlled Bucketwheel	2

ductivity rates than comparable astronaut driven or teleoperated solutions for lunar base construction. This translates into significantly lower total earth-launch mass numbers than astronaut driven or teleoperated approaches. Reduced launch mass was also shown for different vehicle configurations, including a fleet of smaller bulldozer, front loader, and bucket wheel concepts because these solutions achieve higher digging productivity rates with smaller sized vehicles compared with an astronaut-driven configuration. Overall, out of all the alternatives compared, autonomous bulldozing is found to be the most competitive. In terms of number of rocket launches, the multirobot autonomous solutions require up to 50% fewer rocket launches (assuming an Ares V vehicle) than an equivalent astronaut-operated single vehicle excavation solution.

VII. ACKNOWLEDGMENTS

The authors gratefully acknowledge the contribution of the Northern Centre for Advanced Technology Inc. (NORCAT), Electric Vehicle Controllers Ltd. (EVC), the National Science and Engineering Research Council (NSERC), and reviewers' comments.

VIII. APPENDIX

A. Excavation Robot Model

This section includes details outlining the robot model used for ANT controller training and validation using higher fidelity simulations. The the inputs to the ANT controller are shown in Table VII and Figure 21. The robots have access to current (X, Y) from localization scans performed in the simulation. Z (upwards) is computed through integration of changes in depth values. The discretized X and Y coordinates are use to lookup the goal depth $g_{x,y}$ of each grid square region in front of the robot.

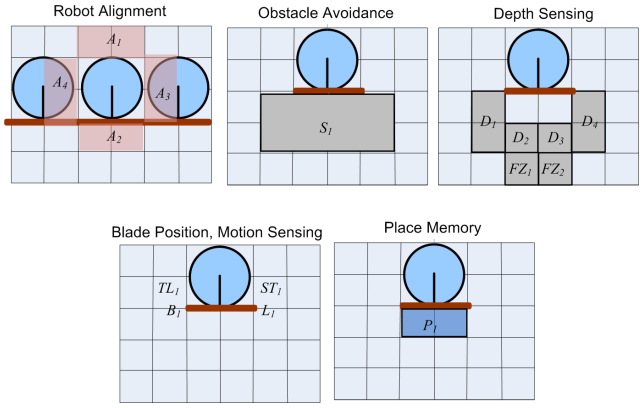

Fig. 21. Robot Input Sensor Mapping for the Simulation Model.

The sensory input and output behaviours mapping for the excavation controller is an extension of the work presented in [4]. This controller can perform coordinated/aligned group actions in addition to the capabilities demonstrated with the previous version of the ANT excavation controller. All raw input data are discretized and fed to the controller. $D_1..D_4$ and $FZ_1..FZ_2$ are obtained using simulated ground scans. In addition a set of simulated IR sensors are used to detect obstacles at the front and back (S_1, S_2). Current X and Y positions of each robot are used to determine the relative position of the nearest robot and are used for wireless communication. Each robot wirelessly communicates by exchanging 1 bit of data between with its nearest neighbouring robot. Alignment sensors ($A_1...A_4$) on the robot are used to determine if neighbouring robots are in alignment position. The Balovnev force feedback for the blade is used to determine BL_1 and orientation data is used to determine TL_1. The robots also have access to one memory bit, which can be manipulated using some of the basis behaviors.

Once two robots are in alignment position and behaviour 2 is triggered (Table VIII), while behaviour 3 is not triggered then the AS_1 value for both robots is set to 1. This group of robots are in aligned state ($AS_1 = 1$) and motor behaviours such as 'move forward', 'turn left' and 'turn right' are performed through consensus (Figure 22). Thus

TABLE VII

ANT CONTROLLER SENSOR INPUTS

Variable	Function	States
$A_1 ... A_4$	Robot Alignment Position	Alignment Position, Not in Alignment Position
$D_1 ... D_4$	Depth Sensing Relative to Goal Depth	Level, Above, Below, Don't Care
FZ_1, FZ_2	Depth Sensing Relative to Ground	Above, Below, Level
B_1	Blade Position	Above, Level, Below Ground, Home
S_1	Front Obstacle Detection	Obstacle, No Obstacle
S_2	Front Obstacle Detection	Obstacle, No Obstacle
TL_1	Robot Tilted Downwards	True, False
ST_1	Robot Stuck	True, False
M_1	Memory bit	0, 1
WC_1	Status of message bit from wireless comm	0, 1
AS_1	Robot Alignment Status	Not Aligned, Aligned
P_1, P_2	Pheromone Concentration relative to $P_{nominal}$	Level, Above, Below

TABLE VIII

ANT CONTROLLER BASIS BEHAVIOURS

Behaviour	Function	States
1	Set Throttle	Set rover throttle to high otherwise remain nominal
2	Want to Align	Intention of rover to go into align state
3	Not Want to Align	Intention of rover to exit out of align state
4	Move Forward	Move one grid square forward
5	Move Backward	Move one grid square backward
6	Random Turn	Randomly Turn 90° right or Turn 90° left
7	Turn Right	Turn 90° right
8	Turn Left	Turn 90° left
9	Blade position: Above	Set blade above ground d cm
10	Blade position: Below	Set blade below ground d cm
11	Blade position: Level	Set blade level to ground
12	Blade position: Home	Retract blade to home position (makes no contact with regolith)
13	Blade Pivot: Nominal	Pivot blade to nominal angle
14	Blade Pivot: Left	Pivot blade 30° (left) from nominal
15	Blade Pivot: Right	Pivot blade -30 ° (right) from nominal
16	Bit Set	Set memory bit 1 to 1
17	Bit Clear	Set memory bit 1 to 0
18	Increment Pheromone	Increment pheromone concentration
19	Decrement Pheromone	Decrement pheromone concentration
20	Wireless Comm.: Send 1	Set message bit 1 to 1 and wirelessly broadcast to nearest rover
21	Wireless Comm.: Send 0	Set message bit 1 to 0 and wirelessly broadcast to nearest rover

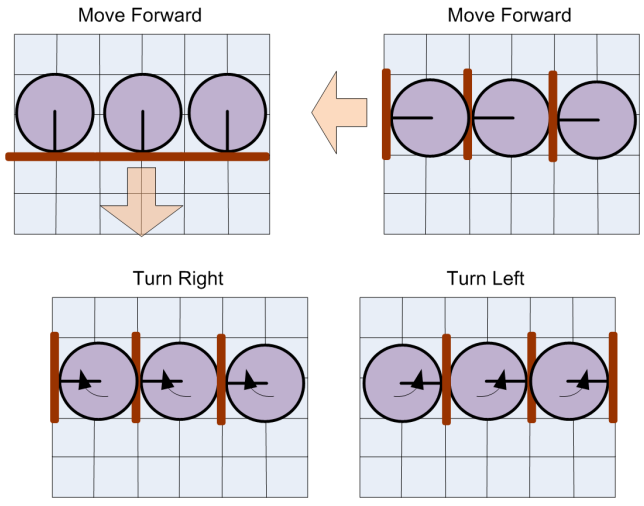

Fig. 22. Robots in aligned state performing various motor behaviors. Note that the 'move forward behavior can be performed in two configurations (side by side and one behind another).

each member of the group has to trigger the 'move forward' behaviour for the group of robots to move forward otherwise the 'move forward' triggered by some members of group are vetoed. Random turns among groups of robots in aligned state implies a synchronized random turn, where all the members 'turn right' or 'turn left' with equal probability. A group of robots detach from aligned state ($AS_1 = 1$) once all members of group trigger behaviour 3 and behaviour 2 is not triggered.

Table VIII lists the basis behaviors the robot can perform (in order) within a single timestep. Darwinian selection is performed based on the fitness value of each controller averaged over 50 different initial conditions, within an 8 X 8 excavation area. The Evolutionary Algorithm population size for the experiments is P = 100, crossover probability p_c = 0.7, mutation probability p_m = 0.025 and tournament size of 0.06 P.

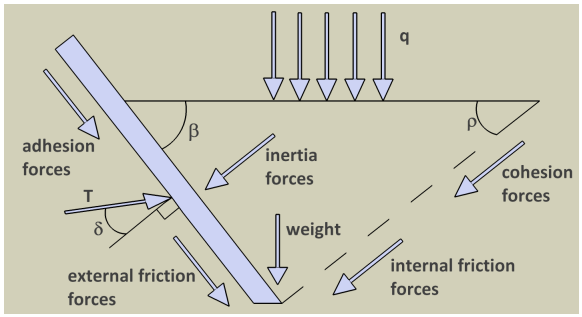

Fig. 23. Cutting Forces of a Flat Blade

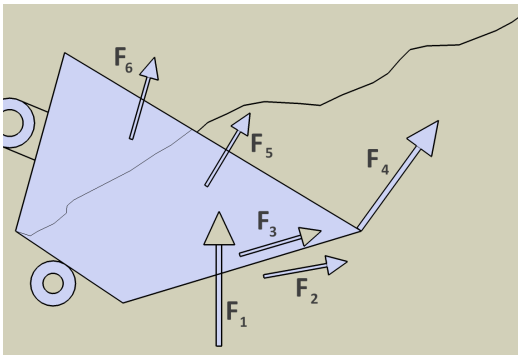

Fig. 24. Forces Exerted by Bucket on Regolith

B. Balovnev Soil Interaction Model

Based on Bolovnev's literature [20], $\mathbf{f_1}$, $\mathbf{f_2}$, $\mathbf{f_5}$ and $\mathbf{f_6}$, shown in Figure 23 are small forces relative to the others. $\mathbf{f_3}$ and $\mathbf{f_4}$ can be broken down into further components.

$$f_{4x} = P_1 + P_2 + P_3 \tag{7}$$

and

$$f_{3x} = P_4 \tag{8}$$

P_1 is both the cutting and surface resistance of sharp edged flat trenching blade, P_2 is resistance posed by bluntness of the edge, P_3 is resistance created from the two bucket sides, P_4 is frictional resistance on those sides. Additional parameters are shown in Figure 24. Horizontal force is now found to be:

$$\begin{aligned} H &= (P_1 + P_2 + P_3) + P_4 \\ &= wd(1 + \cot\beta\cot\delta)A_1 \\ &\quad \cdot \left(\frac{dg\gamma}{2} + c\cot\phi + gq + BURIED \star (d - l\sin\beta)\right. \\ &\quad \left. \cdot \left(g\gamma\frac{1-\sin\phi}{1+\sin\phi}\right)\right) + we_b(1 + \tan\delta\cot\alpha_b)A_2 \\ &\quad \cdot \left(\frac{e_b g\gamma}{2} + c\cot\phi + gq + dg\gamma\left(\frac{1-\sin\phi}{1+\sin\phi}\right)\right) + \\ &\quad 2sdA_3\left(\frac{dg\gamma}{2} + c\cot\phi + gq + BURIED\right. \\ &\quad \left. \star(d - l_s\sin\beta)\left(g\gamma\frac{1-\sin\phi}{1+\sin\phi}\right)\right) + 4\tan\delta A_4 l_s d \end{aligned}$$

TABLE IX
LIST OF BALOVNEV PARAMETERS

Tool Width	w
Tool Length	l
Tool Depth	d
Side Length	l_s
Side Thickness	s
Blunt Edge Angle	α_b
Blunt Edge Thickness	e_b
MOON gravity	g_M
Regolith Specific Mass	γ
Surcharge Mass	q
Rake Angle	β
Cohesion	c
Internal Friction Angle	ϕ
External Friction Angle	δ

$$\cdot \left(\frac{dg\gamma}{2} + c\cot\phi + gq + BURIED \star (d - l_s\sin\beta)\left(g\gamma\frac{1-\sin\phi}{1+\sin\phi}\right)\right) \tag{9}$$

with $BURIED = TRUE$ or $FALSE$ being 1 or 0 based on whether or not the entire bucket is submerged into the regolith. Geometric factors that consider the srace angle relative to the plane of reference are$A_1 = A(\beta), A_2 = A(\alpha_b), A_3 = A_4 = A\left(\frac{\pi}{2}\right)$. For A_i, β and α_b the following equation can be used:

$$A(\beta) = \begin{cases} \frac{1-\sin\phi\cos 2\beta}{1-\sin\phi} \\ \quad \text{if } \beta < 0.5\left[\sin^{-1}\left(\frac{\sin\delta}{\sin\phi}\right) - \delta\right] \\ \frac{\cos\delta(\cos\delta + \sqrt{\sin^2\phi - \sin^2\delta})}{1-\sin\phi} e^{[2\beta - \pi + \delta + \sin^{-1}\left(\frac{\sin\delta}{\sin\phi}\right)]\tan\phi} \\ \quad \text{if } \beta \geq 0.5\left[\sin^{-1}\left(\frac{\sin\delta}{\sin\phi}\right) - \delta\right] \end{cases}$$

Total and Vertical force is now:

$$T = H\csc(\beta + \delta) \tag{10}$$

$$V = H\cot(\beta + \delta) \tag{11}$$

REFERENCES

[1] Mau, S. and Dolan, J., "Scheduling for Humans in Multirobot Supervisory Control," *in proceedings of IEEE/RSJ International Conference on Intelligent Robotic Systems, IEEE*, Washington DC, 2007.

[2] Boles, W. W., David, B. A., and Tucker, R. L., "Lunar Base Construction Equipment and Methods Evaluation," *Journal of Aerospace Engineering*, 1993.

[3] Thangavelautham, J. and D'Eleuterio, G. M. T., "A Coarse-Coding Framework for a Gene-Regulatory-Based Artificial Neural Tissue," *in Advances In Artificial Life: Proceedings of the 8th European Conference on ALife*, Springer, Berlin, 2005, pp. 67–77.

[4] Thangavelautham, J., Smith, A., Samid, N. A. E., Ho, A., Boucher, D., Richard, J., and D'Eleuterio, G. M. T., ""Multirobot Lunar Excavation and ISRU Using Artificial-Neural-Tissue Controllers "," *Space Technology and Applications International Forum—STAIF*, Feb 2008.

[5] Thangavelautham, J., Smith, A., Boucher, D., Richard, J., and D'Eleuterio, G. M. T., ""Evolving a Scalable Multirobot Controller Using an Artificial Neural Tissue Paradigm"," *IEEE International Conference on Robotics and Automation*, April 2007.

[6] Corporation, D. S. and Studios, D., "Realime 3D Open Source Digital Spaces Simulation Software," .

TABLE X

LIST OF LAUNCH MASS AND PROBABILITY DISTRIBUTION PARAMETERS

a	lower limit of beta distribution
b	upper limit of beta distribution
x	independent variable of beta distribution
K	normalizing constant of beta distribution
m	most likely value of beta distribution
M_i	mass of machine/attachment i
$\#_i$	number of machines/attachments i
C_i	number of machines/attachments i consumed
$INT(value)$	"value" rounded up to nearest whole number
R_i	maintenance resupply mass for machine/attachment i
EVA	number of EVA hours used for construction operations
IVA	number of IVA hours used for construction operations
$MEVA_i$	maintenance EVA hours for machine/attachment i
$MIVA_i$	maintenance IVA hours for machine/attachment i
$REVA_i$	rebuild EVA hours for required for machine i
$RIVA_i$	rebuild IVA hours for required for machine i
H_{EVA}	productive number of EVA hours per day per crew member
H_{IVA}	productive number of IVA hours per day per crew member
D	number of days per week
M_D	crew-consumables mass per crew member per day
Q_j	quantity of work for task j
P_j	productivity for task j
N_{ij}	number of machines i assigned to task j
$Life_i$	operational life of machine i
$A\%_{ij}$	percent of task duration machine i is assigned to task j
$NEVA_j$	number of EVA crew assigned to task j
$A\%EVA_j$	percent of task duration EVA crew is assigned to task j
$NIVA_j$	number of IVA crew assigned to task j
$A\%IVA_j$	percent of task duration IVA crew is assigned to task j
α, β	shape parameters of beta distribution
$\hat{\mu}$	expected value of beta distribution

[7] Newman, P., "Personal Communication," Digital Spaces Forum, 2007-2008.

[8] Matsumoto, S., Yoshida, T., K. H., and Takagi, K., "Constuction Engineering Approach for Lunar Base Development," *Journal of Aerospace Engineering*, 1998, pp. 129–137.

[9] Armstrong, K., McAdams, D. A., and Norrell, J. L., "Conceptual Design of a Fleet of Autonomous Regolith Throwing Devices for Radiation Shielding of Lunar Habitats (Supplemental Report)," Tech. rep., NASA Technical Reports Server, 1992.

[10] Mikulas, M., "Lunar Surface Structural Concepts and Construction Studies," *Center for Space Construction Third Annual Symposium*, 1991.

[11] Mueller, R. P. and King, R. H., "Trade Study of Excavation Tools and Equipment for Lunar Trade Study of Excavation Tools and Equipment for Lunar Outpost Development and ISRU," *Space Technology and Applications International Forum—STAIF*, 2008.

[12] Richardson-Little, W. W. and Damaren, C. J., "Position Accommodation and Compliance Control for Robotic Excavation," *IEEE International Conference on Control Applications*, Vol. 2, 2005, pp. 1194–1199.

[13] Bristow, K. L. and Holt, J. A., "Can Termites Create Local Energy Sinks to Regulate Mound Temperature," *Journal of Thermal Biology*, Vol. 12, 1997, pp. 19–21.

[14] Brooks, R. A., Maes, P., and Mataric, M. J., "Lunar Base Construction Robots," *IEEE International Workshop on Intelligent Robots and Systems*, Vol. 1, 1990, pp. 389–392.

[15] NASA-1, "Exploration Studies Technical Report, FY-89 Status," Tech. rep., NASA Office of Exploration, 1989.

[16] Corporation, D. S. and Studios, D., "Shackleton Crater and Highlander Rover," .

[17] Littlefield, T. and Randolph, P., ""An Answer to Sasieni's Question on PERT Times"," *Management Science*, Vol. 33, No. 10, October 1987.

[18] Abuelsamid, N., *Lunar Excavation Methods and Evaluation*, Master's thesis, Univeristy of Toronto Institute for Aerospace Studies, 2008.

[19] "Constellation Program: America's Fleet of Next-Generation Launch Vehicles, The Ares V Cargo Launch Vehicle," Tech. rep., National Aeronautics and Space Administration, 2008.

[20] Balovnev, V. I., *New Methods for Calculating Resistance to Cutting of Soil*, Amerind Publishing (Trans- lation), Available from National Technical Information Service, Springfield, VA 22161, 1983.